Asian Journal of Chemistry; Vol. 37, No. 8 (2025), 1867-1872

ASIAN JOURNAL OF CHEMISTRY

https://doi.org/10.14233/ajchem.2025.34001

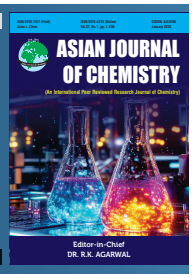

Ag/Cu-Fe_3O_4 Nanocomposite Catalyzed Chemoselective Reduction of Nitroarenes to Aminoarenes

S. Ghadage[1], K. Shelar[1], P. Sarvalkar[1], A. Sawant[2], Y. Patil[1], T. Bhat[1] and S. Sawant[1,*]

[1]School of Nanoscience and Biotechnology, Shivaji University, Kolhapur-416004, India
[2]School of Chemical Sciences, Sanjay Ghodawat University, Atigre, Kolhapur-416008, India

*Corresponding author: E-mail: sas.snst@unishivaji.ac.in

Received: 6 May 2025; *Accepted*: 28 June 2025; *Published online*: 31 July 2025; AJC-22063

This study reports the synthesis of Ag/Cu-Fe_3O_4 nanocomposite, using a naturally occurring amino acid L-arginine as a linker and its catalytic application to reduce nitroaromatic compounds to aminoaromatic compounds. Decoration of Cu and Ag nanoparticles on Fe_3O_4 NPs created the Ag/Cu-Fe_3O_4 nanocomposite. Advanced characterization techniques confirmed the composition and morphology of the synthesized nanocomposite. The catalytic performance of Ag/Cu-Fe_3O_4 nanocomposite was evaluated using UV-visible spectrophotometry for $NaBH_4$ assisted reduction of 4-nitrophenol to 4-aminophenol and 5-nitroisophthalic acid to 5-aminoisophthalic acid. After multiple cycles, results demonstrated that nanocomposite facilitates rapid and efficient chemical transformations with high selectivity and over 80% efficiency. Additionally, the nanocomposite's capability for easy magnetic recovery and recyclability underscores its potential as a cost-effective and environmentally friendly solution for industrial applications in sensing, catalysis and green chemistry. This work presents a novel strategy for converting nitroarenes to aminoarenes, leveraging unique synergetic properties of Ag/Cu-Fe_3O_4 nanocomposite.

Keywords: Ag/Cu-Fe_3O_4, Nanocomposite, Nitroarenes reduction, Catalytic reduction, Nanocatalysis.

INTRODUCTION

In organic chemistry, reduction of nitroaromatics to their respective amino aromatics is one of the fundamental reactions. These amino derivatives have commercial importance in the production of dyes, agrochemicals, pharmaceuticals and fine chemicals [1,2]. With recent surge in nanochemistry, there has been interesting advancements in this important reaction of reduction of nitroaromatics [3]. Different catalysts have been reported for catalytic reduction of nitro compound such as Fe_3O_4 NPs [4], Fe_3O_4@SN/GLA@chitosan-Ag [5], Au/TiO_2 or Au/Fe_2O_3, Au/MgO, Au/mesoporous TiO_2, Au-Pd/Al_2O_3, Pd/C, biomass-based Ag, porous silica encapsulated Rh NPs, Ru/rGO, nitrogen and oxygen doped carbon, Fe_3O_4@Al_2O_3, Pd NPs supported on carbon nitride, Pt NPs/clusters, ultra-dispersed nickel phosphide on phosphorus doped carbon and oxygen-deficient tungsten oxides, *etc*. [6-18]. Among them magnetic nanoparticles based on Fe NPs have emerged as a conventional catalyst material [19,20]. They can be easily separated from the reaction system by manipulating the external magnetic field. Combination of the Fe magnetic nanoparticles along with other metals like Ni, Cu, Ag, Ti, Au, *etc*. enhances the catalytic activity [21,22]. Silver and Cu NPs along with $NaBH_4$ as a reducing agent can independently catalyze reduction of nitro compounds to amines and shows good catalytic activity [22,23]. But there is problem of easy recovery of these catalysts for recyclability since both the materials cannot be recovered by magnetic field. Fe_3O_4 magnetic nanoparticles in combination either with Ag or Cu exhibited excellent catalytic activity for reduction of 4-nitrophenol to 4-aminophenol [24,25].

4-Nitrophenol is a precursor of 4-amino phenol, which is used in manufacturing of pharmaceutical drugs and pesticides. Due to its toxic, carcinogenic and corrosive properties, it must be degraded or eliminated in some applications [26], and it can be converted to 4-aminophenol, a crucial intermedite in the synthesis of analgesic and antipyretic drugs. Similarly, 5-aminoisophthalic acid (5-AIPA) is used as the raw material or intermediate in organic synthesis, used as X-ray contrast agent, environmental remediation [27], catalysis, *etc*. As per literature survey it was observed that only few methods are available for synthesis of 5-AIPA [28,29].

Based on the recent research works, as earth abundant and magnetically separable Fe_3O_4 based catalysts [29,30], devel-

opment of template for morphological tuning of nanomaterials [31,32] and functionalization of molecules for specific applications [33,34] and considering need of use of bio-based materials, a catalyst for reduction of nitroarenes is developed. In present work, emphasis is given on the chemoselective reduction of 4-nitrophenol and 5-nitroisophthalic acid (5-NIPA) to 4-aminophenol and 5-aminoisophthalic acid (5-AIPA), respectively in the presence of AgCu-Fe_3O_4 nanocomposite and $NaBH_4$ by using UV spectrophotometric method. The composite material is prepared by using L-arginine, an amino acid and choice of L-arginine is based on the previous findings [29]. Moreover, L-arginine has electron rich amino sites that has affinity for metal ions such as Ag^+ and Cu^{2+} [35].

EXPERIMENTAL

Anhydrous ferric chloride (98%), potassium iodide, ammonia solution (NH_4OH, 30% v/v) were obtained from Thomas Baker Pvt. Ltd., Mumbai, India. L-Arginine, silver nitrate, copper(II) nitrate, 4-nitrophenol, sodium borohydride and 5-nitroisophthalic acid (5-NIPA, 98%) were purchased from Sigma-Aldrich, USA. All the chemicals were of reagent grade and used without any purification. For all the experiments, deionized water was used.

Instrumentation: The crystalline structures present in the samples were analyzed with X-ray diffraction (XRD). The analysis was carried out using a high-precision Bruker D2 Phaser X-ray diffractometer. The instrument utilized Cu*K*α radiation, having a wavelength of 1.542 Å, which is particularly effective for penetrating and diffracting through the crystalline material to provide detailed diffraction patterns. Field emission electron microscope (FESEM) (JEOL) was used to examine the surface morphology. This microscope is capable of operating at a wide range of accelerating voltages from 0.1 kV to 30 kV and allows for high-resolution imaging of the surfaces of samples. The UV-Vis spectrophotometer (Agilent Technologies, Cary 60 model), was used to monitor the conversion process.

Synthesis of Fe_3O_4 NPs: The Fe_3O_4 NPs were synthesized following a reported method. Initially, 4.86 g (0.0299 M) of anhydrous $FeCl_3$ dissolved in 40 mL of distilled water was added to KI (1.64 g, 0.0098 M) solution while stirring the solution at room temperature for 1 h. Following this, the mixture underwent sonication for 30 min to enhance the reaction kinetics. Following the sonication, the solution was filter to eliminate the iodine precipitate. Then, the filtrate was treated with 30% v/v NH_4OH, added dropwise and stirring vigorously until the pH reached between 10 and 13, which led to the complete precipitation of black magnetite NPs. The precipitate was washed with distilled water until the pH stabilized at 7 and subsequently dried at 70 ºC for 10 h to obtain the Fe_3O_4 NPs. These NPs were then utilized in the subsequent synthesis of Ag/Cu-Fe_3O_4 nanocomposite.

Synthesis of Ag/Cu-Fe_3O_4 nanocomposite: To synthesize Ag/Cu-Fe_3O_4 nanocomposite, 25 mg Fe_3O_4 NPs were dispersed in 25 mL of distilled water followed by the addition of 0.25 g of L-arginine solution. To ensure through mixing, the mixture was sonicated for 30 min. To remove any unbound L-arginine, the mixture was washed three times with distilled water. The functionalized nanoparticles were then redispersed in distilled water. To this dispersion, 1.6 mM of $AgNO_3$ and 1.6 mM of $Cu(NO_3)_2$ were added followed by rapid introduction of 0.6 g of $NaBH_4$ in order to start the reduction process. To ensure the reaction was complete, the reaction mixture was continuously stirred for 30 min. The reaction mixture was centrifuged at 6000 rpm for 10 min to separate the nanoparticles. The collected particles were washed with ethanol to eliminate any remaining reactants and byproducts. Finally, the nanoparticles were vacuum dried at 80 ºC to obtain Ag/Cu-Fe_3O_4 nanocomposite.

Reduction of 4-nitrophenol and 5-nitroisophthalic acid (5-NIPA) assay: In a typical experiment, 1.5 mL of nitroarene was mixed with 500 µL of 5×10^{-2} M $NaBH_4$ solution in the cuvette. Following this, 100 µL of Ag/Cu-Fe_3O_4 nanocomposite suspension (0.2 mg/mL) was added to the above solution. The yellow colour of solution gradually disappeared, confirmed the reduction of 4-nitrophenol. The concentration of 4-nitrophenol was determined with UV-visible spectroscopy at the wavelength of 400 nm.

RESULTS AND DISCUSSION

XRD studies: Using an X-ray diffractometer with a 1.54 Å wavelength, distinct diffraction peaks were captured and analyzed. The peaks (Fig. 1) correspond to the specific planes characteristic of Fe_3O_4, Cu and Ag NPs, confirmed their coexistence in the nanocomposite. Specifically, the diffraction peaks at 2θ of 32.47º, 35.50º, 43.33º, 53.82º and 62.86º aligned with the (220), (311), (400), (422) and (440) planes, respectively, confirmed the presence of Fe_3O_4 NPs as indexed in the ICSD (250,540). Furthermore, additional peaks at 2θ = 43.33º, 50.22º and 74.41º were observed, which match the (111) and (311) planes associated with Cu NPs, as per the JCPDS (71-4610). Similarly, Ag NPs exhibited peaks at 2θ = 38.12º, 43.33º, 64.42º and 77.30º, which correspond to the (111), (200), (220) and (311) planes (JCPDS: 04-0783). Notably, the peak at 43.33º is a shared feature among Fe_3O_4, Cu and Ag, illustrating the overlapping nature of these crystal-line structures within the nanocomposite. This over-

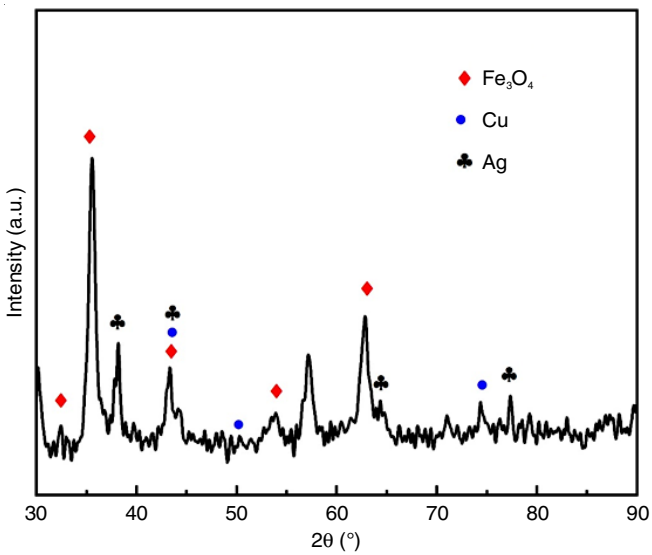

Fig. 1. XRD spectra of Ag/Cu-Fe_3O_4 nanocomposite

lapping indicates a potential interaction between the different metal and oxide components at the nanoscale, which may influence the physical and chemical properties of the nanoparticles. The Debye-Scherrer's formula revealed an average size of 5.5 nm for the nanoparticles, which confirms the high degree of uniformity in the particle size distribution.

Morphological studies: Fig. 2 presents FESEM images of the Ag/Cu-Fe_3O_4 nanocomposites, illustrating their morphology and size distribution. These images distinctly illustrate the formation of nanocomposites, which are relatively spherical in shape. These nanocomposites tend to agglomerate, forming clusters, which appear as grouped or clustered spheres. This characteristic agglomeration suggests interactions between the particles that lead to their collective assembly [36]. The uniform spherical shape is useful in applications such as catalysis, where the surface area and symmetry of the nanoparticles can have a significant impact on the catalytic activity. Moreover, the spherical structure may enhance the physical stability and dispersion of nanoparticles in solutions [37].

Catalytic performances of Ag/Cu-Fe_3O_4 nanocomposite: The UV-visible absorption spectra (Fig. 3a) initially identify the absorption peak of 4-nitrophenol at 315 nm, a characteristic peak indicating the presence of 4-nitrophenol in solution (pale yellow). The addition of $NaBH_4$ causes this peak to shift to 400 nm, signifying the formation of 4-nitrophenolate ions in a basic medium (solution turns yellow). It is known that the solution turns yellow due to formation of *p*-nitrophenolate ions [25]. In control experiment, when this solution was held for 2 h without adding catalyst, the peak at 400 nm remained as such indicating that $NaBH_4$ alone cannot drive the reduction reaction of 4-nitrophenol. After introducing the Ag/Cu-Fe_3O_4 nanocomposite as catalyst, there is a notable decrease in the intensity of peak at 400 nm, followed by the appearance of a new peak at 300 nm (solution become colourless). The process reaches completion in 13 min, which is significantly rapid, highlighting the efficiency of the nanocomposite catalyst. The rate constant k of 0.1707 min^{-1}, calculated from the reaction kinetics depicted in Fig. 3b, further highlights the high activity and effectiveness of catalyst.

The catalyst was found to be active and effective when compared with previously reported catalysts. The comparison of selected catalysts with present catalyst based on its application in the reduction of 4-nitrophenol to 4-aminophenol using $NaBH_4$ is summarized in Table-1.

Similarly, the reduction of 5-nitroisophthalic acid (5-NIPA) was analyzed through UV-visible spectroscopy (Fig. 3c). The initial absorption peak at 260 nm shifts to 300 nm upon adding $NaBH_4$, denoting the formation of 5-nitroisophthalate ions. Consistent with the 4-nitrophenol experiment, the 300 nm peak remains unchanged without the catalyst, illustrating that $NaBH_4$ alone does not facilitate the reduction of 5-NIPA. The addition of Ag/Cu-Fe_3O_4 nanocomposite causes a gradual decline in the

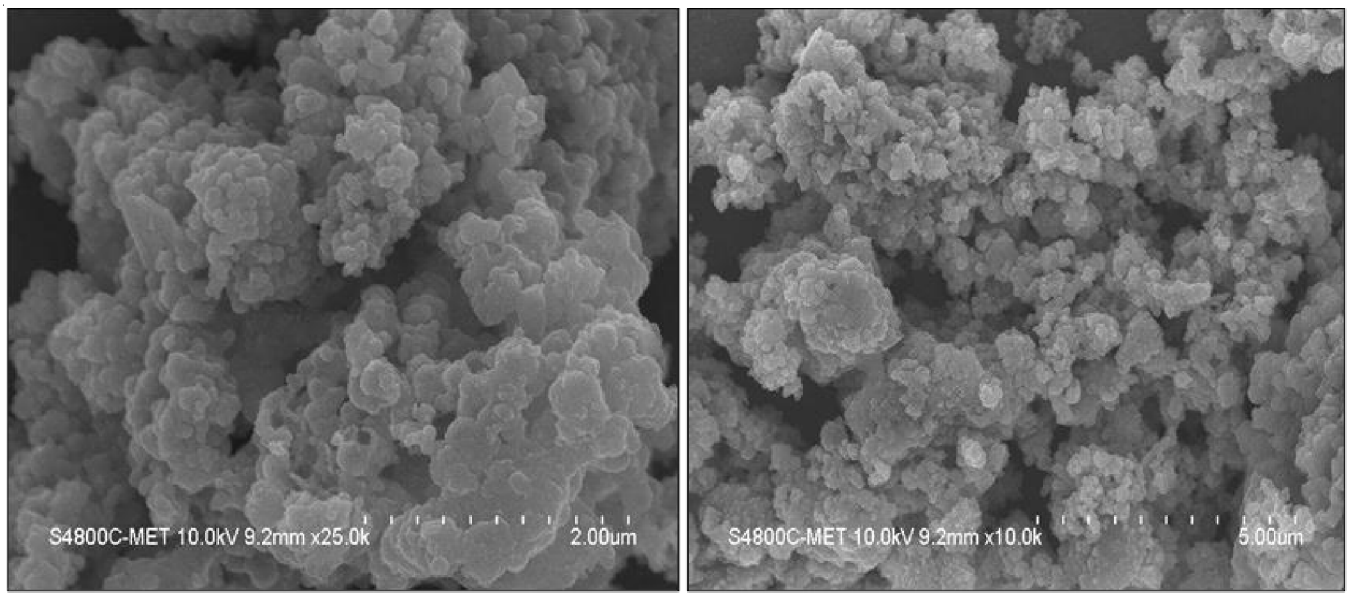

Fig. 2. FESEM images of Ag/Cu-Fe_3O_4 nanocomposite

TABLE-1
COMPARATIVE ACCOUNT OF REPORTED CATALYSTS FOR REDUCTION OF 4-NITROPHENOL TO 4-AMINOPHENOL

Catalyst	Conversion (%)	Time (min)	Reaction conditions	Ref.
Catalyst	100	13	RT, air	Present study
Au-Fe_3O_4	100	10	RT, air	[38]
Fe_3O_4@SN/GLA@chitosan-Ag	100	3	RT, under N_2	[5]
NAP-Mg–Au(0)	100	7	RT, air	[6]
Wood-nanomaterial supported Pt NPs	> 90	10	RT, air	[17]
Cu/Fe_3O_4 NPs	100	4	RT, under N_2	[19]
Ag/Cu@Fe_3O_4	100	–	RT, air	[25]

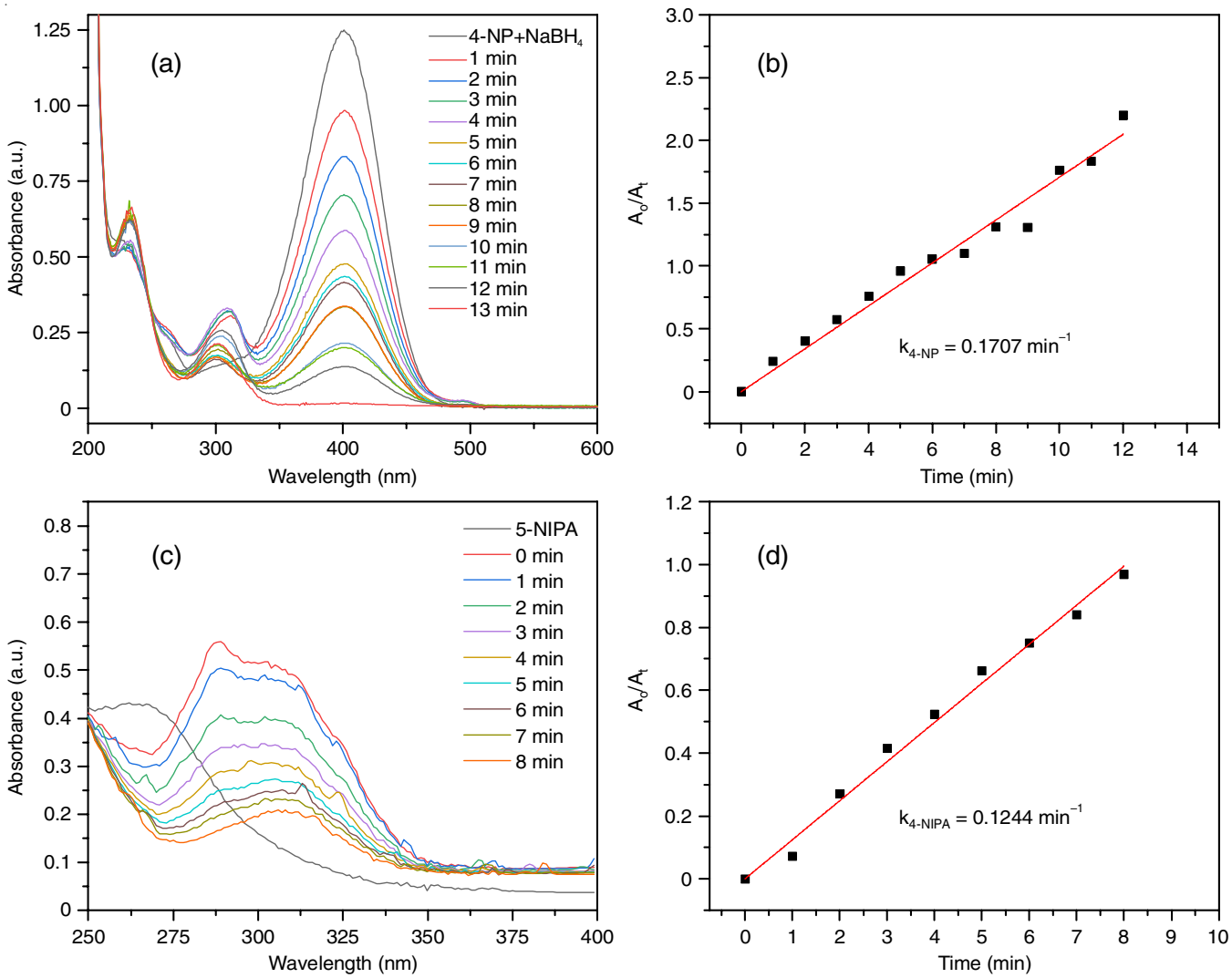

Fig. 3. (a) UV-visible absorption spectra for the reduction of 4-nitrophenol (4-NP), (b) reaction kinetics for the catalytic reduction of 4-nitrophenol in the presence of Ag/Cu-Fe_3O_4 nanocomposite, (c) UV-visible absorption spectra for the reduction of 5-NIPA and (d) reaction kinetics for the catalytic reduction of 5-NIPA in the presence of Ag/Cu-Fe_3O_4 nanocomposite

300 nm peak, with complete conversion to 5-aminoisophthalic acid (5-AIPA) observed within 8 min. This rapid and efficient reduction, completed in 8 min with a rate constant k of 0.1244 min^{-1}, as shown in Fig. 3d, demonstrates the selectivity and efficiency of catalyst. This rapid conversion can be attributed to the synergistic effect of Cu and Ag. Interesting to observe that in control experiment when reduction was attempted using only $NaBH_4$ or in presence of Fe_3O_4 NPs, no conversion was observed in case of both the substrates.

The chemo-selectivity of the catalyst, particularly its ability to target and reduce specific nitro compounds to their corresponding amines without over-reduction or side reactions, is of significant interest. The unique surface properties and electron transfer capabilities of Ag/Cu-Fe_3O_4 nanocomposite, which merit further studies to fully elucidate the underlying mechanisms, could be responsible for this specificity. Furthermore, the simple and potentially scalable method used to synthesize the Ag/Cu-Fe_3O_4 nanocomposite suggests its practical applicability in industrial processes, offering a sustainable and cost-effective solution for the treatment of pollutants and the synthesis of valuable compounds [32,33].

Reaction mechanism of catalytic reduction of nitroarenes

Reduction of 4-nitrophenol: The Langmuir-Hinshelwood mechanism facilitates the reduction of 4-nitrophenol to 4-aminophenol, involving the adsorption of 4-nitrophenol molecules onto the surface of Ag/Cu-Fe_3O_4 nanocomposite (**Scheme-I**). In this catalyzed reaction, $NaBH_4$ serves as the hydrogen donor. The interaction starts with a colour change from pale-yellow to bright yellow upon the formation of nitrophenolate anions under alkaline conditions. A notable redshift in the absorption peak to 400 nm occurs upon adding $NaBH_4$, indicating the progression of the reduction. As the reaction continues in the presence of catalyst, the peak at 400 nm decreases and a new peak at 300 nm appears, signaling the formation of colourless 4-aminophenol. The complete transformation is evidenced by the appearance of two isosbestic points at 311 and 280 nm. The process involves electron transfer from BH_4^- to 4-nitro-

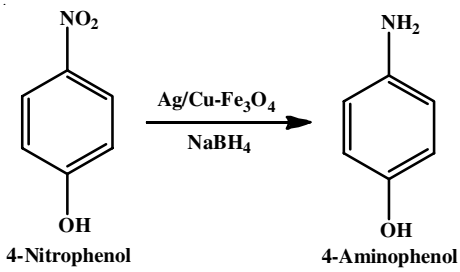

Scheme-I: Reduction of 4-nitrophenol to 4-aminophenol in presence of Ag/Cu-Fe_3O_4 nanocomposite

phenol facilitated by the metal nanoparticles, leading to the reduction of the nitro group to an amino group through intermediate stages, including the formation of a dihydroxy-like structure and subsequent dehydration to form 4-aminophenol [29,30,32].

Reduction of 5-NIPA to 5-AIPA: It is inferred that a similar Langmuir-Hinshelwood mechanism applies to the reduction mechanism for 5-NIPA (**Scheme-II**). 5-NIPA adsorbed onto the Ag/Cu-Fe_3O_4 nanocomposite surface and $NaBH_4$ would act as reducing agent, donating electrons and hydrogen atoms necessary for the conversion of the nitro group to an amino group. The reaction follows a pathway involving the formation of an intermediate species, reduction of the nitro group and stabilization of the final product, 5-AIPA, all facilitated by the catalytic action of the nanocomposite. This process was monitored by changes in the UV-visible spectra, which indicate whether the reaction is progressed or finished.

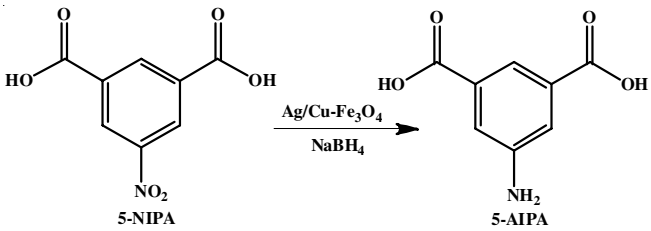

Scheme-II: Reduction of 5-NIPA to 5-AIPA in presence of Ag/Cu-Fe_3O_4 nanocomposite

Recyclability study: An efficient nanocatalyst should have a larger adsorption capacity and better desorption efficiency, resulting in lower costs for the nanocatalyst. Using a magnet, the Ag/Cu-Fe_3O_4 nanocomposite was recovered. After the catalytic reactions, one can separate the particles for the next cycle. Fig. 4 shows that even after four cycles, the Ag/Cu-Fe_3O_4 nanocomposite reduced nitroarenes with an efficiency of more than 90%. Compared to the first run, during the first cycle, it demonstrated more than 90% catalytic activity. Therefore, its magnetic nature enables easy recovery and reuse, maintaining the same catalytic activity for at least four cycles.

Conclusion

In this study, Ag/Cu-Fe_3O_4 nanocomposite was successfully synthesized by chemical reduction method by using naturally occurring amino acid L-arginine as linker. The morphological studies of synthesized Ag/Cu-Fe_3O_4 nanocomposite shows the relatively spherical shape with the agglomerated particles. The

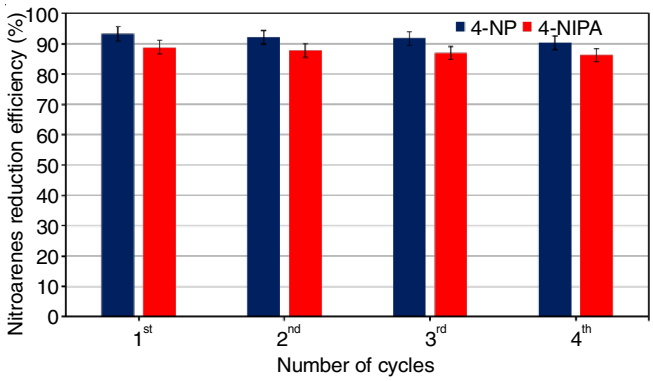

Fig. 4. Recyclability study of nitroarenes reduction efficiency on Ag/Cu-Fe_3O_4 nanocomposite

Ag/Cu-Fe_3O_4 nanocomposite is found to be a highly efficient and selective catalyst in the reduction of nitroaromatic compounds, as demonstrated in the catalytic performance studies. The reduction of 4-nitrophenol to 4-aminophenol was completed in 13 min with a rate constant of 0.1707 min^{-1}, indicating the rapid and effective catalytic activity of nanocomposite. Similarly, the reduction of 5-nitroisophthalic acid (5-NIPA) to 5-aminoisophthalic acid (5-AIPA) occurred within 8 min, achieving a rate constant of 0.1244 min^{-1}. These findings emphasize the nanocomposite's capability to facilitate swift and efficient chemical transformations, making it suitable for applications in environmental remediation and chemical synthesis. Moreover, the nanocomposite's structure enables effective recyclability and reuse, maintaining over 85% of its catalytic activity after four cycles, which enhances its sustainability and cost-effectiveness for continuous industrial processes.

ACKNOWLEDGEMENTS

Authors wish to acknowledge School of Nanoscience and Biotechnology, Shivaji University, Kolhapur for laboratory and characterization support.

CONFLICT OF INTEREST

The authors declare that there is no conflict of interests regarding the publication of this article.

REFERENCES

1. A.M. Tafesh and J. Weiguny, *Chem. Rev.*, **96**, 2035 (1996); https://doi.org/10.1021/cr950083f
2. R.S. Downing, P.J. Kunkeler and H. Van Bekkum, *Catal. Today*, **37**, 121 (1997); https://doi.org/10.1016/S0920-5861(97)00005-9
3. H.K. Kadam and S.G. Tilve, *RSC Adv.*, **5**, 83391 (2015); https://doi.org/10.1039/C5RA10076C
4. S. Kim, E. Kim and B.M. Kim, *Chem. Asian J.*, **6**, 1921 (2011); https://doi.org/10.1002/asia.201100311
5. Z.-Z. Wang, S.-R. Zhai, B. Zhai, Q.-D. An and S.-W. Li, *J. Sol-Gel Sci. Technol.*, **75**, 680 (2015); https://doi.org/10.1007/s10971-015-3738-9
6. H.U. Blaser, *Science*, **313**, 312 (2006); https://doi.org/10.1126/science.1131574
7. K. Layek, M.L. Kantam, M. Shirai, D. Nishio-Hamane, T. Sasaki and H. Maheswaran, *Green Chem.*, **14**, 3164 (2012); https://doi.org/10.1039/c2gc35917k

8. S. Fountoulaki, V. Daikopoulou, P.L. Gkizis, I. Tamiolakis, G.S. Armatas and I.N. Lykakis, *ACS Catal.*, **4**, 3504 (2014); https://doi.org/10.1021/cs500379u
9. Y. Xiang, Q. Meng, X. Li and J. Wang, *Chem. Commun.*, **46**, 5918 (2010); https://doi.org/10.1039/c0cc00531b
10. F. Li, B. Frett and H.Y. Li, *Synlett*, **25**, 1403 (2014); https://doi.org/10.1055/s-0033-1339025
11. C. Gao, Q. An, Z. Xiao, S. Zhai, B. Zhai and Z. Shi, *Carbohydr. Polym.*, **181**, 744 (2018); https://doi.org/10.1016/j.carbpol.2017.11.083
12. L. Liu, J. Li, Y. Ai, Y. Liu, J. Xiong, H. Wang, Y. Qiao, W. Liu, S. Tan, S. Feng, K. Wang, H. Sun and Q. Liang, *Green Chem.*, **21**, 1390 (2019); https://doi.org/10.1039/C8GC03595D
13. Y. Duan, M. Zheng, D. Li, D. Deng, L. Ma and Y. Yang, *Green Chem.*, **19**, 5103 (2017); https://doi.org/10.1039/C7GC02310C
14. S. Fujita, H. Watanabe, A. Katagiri, H. Yoshida and M. Arai, *J. Mol. Catal. Chem.*, **393**, 257 (2014); https://doi.org/10.1016/j.molcata.2014.06.021
15. M. Moghaddam, B. Pieber, T. Glasnov and C. Kappe, *ChemSusChem*, **7**, 3122 (2014); https://doi.org/10.1002/cssc.201402455
16. D. Nandi, S. Siwal, M. Choudhary and K. Mallick, *Appl. Catal. A Gen.*, **523**, 31 (2016); https://doi.org/10.1016/j.apcata.2016.04.004
17. X. Lin, M. Wu, D. Wu, S. Kuga, T. Endo and Y. Huang, *Green Chem.*, **13**, 283 (2011); https://doi.org/10.1039/C0GC00513D
18. R. Gao, L. Pan, H. Wang, X. Zhang, L. Wang and J. Zou, *ACS Catal.*, **8**, 8420 (2018); https://doi.org/10.1021/acscatal.8b02091
19. Z. Wang, S. Zai, J. Lv, H. Qi, W. Zheng, B. Zhai and Q. An, *RSC Adv.*, **5**, 71575 (2015).
20. P. Baumeister, H. Blaser and M. Studer, *Catal. Lett.*, **49**, 219 (1997); https://doi.org/10.1023/A:1019034128024
21. Z. Wang, S. Zhai, B. Zhai and Q. An, *Eur. J. Inorg. Chem.*, **2015**, 1692 (2015); https://doi.org/10.1002/ejic.201403219
22. N. Pradhan, A. Pal and T. Pal, *Colloids Surf. A Physicochem. Eng. Asp.*, **196**, 247 (2002); https://doi.org/10.1016/S0927-7757(01)01040-8
23. D. Patil, J. Manjanna, S. Chikkamath, V. Uppar and M. Chougala, *J. Hazard. Mater. Adv.*, **4**, 100032 (2021); https://doi.org/10.1016/j.hazadv.2021.100032
24. A. Vu, H. Le, T. Phan and H. Le, *Polymers*, **15**, 3373 (2023); https://doi.org/10.3390/polym15163373
25. Y. Zhang, W. Yan, Z. Sun, X. Li and J. Gao, *RSC Adv.*, **4**, 38040 (2014); https://doi.org/10.1039/C4RA05514D
26. G. Eichenbaum, M. Johnson, D. Kirkland, P. O'Neill, S. Stellar, J. Bielawne, R. DeWire, D. Areia, S. Bryant, S. Weiner, D. Desai-Krieger, P. Guzzie-Peck, D.C. Evans and A. Tonelli, *Regul. Toxicol. Pharmacol.*, **55**, 33 (2009); https://doi.org/10.1016/j.yrtph.2009.05.018
27. W.-Q. Xu, S. He, S.-J. Liu, X.-H. Liu, Y.-X. Qiu, W.-T. Liu, X.-J. Liu, L.-C. Jiang and J.-J. Jiang, *Inorg. Chem. Commun.*, **108**, 107515 (2019); https://doi.org/10.1016/j.inoche.2019.107515
28. A. Patra, A. Dutta and A. Bhaumik, *Catal. Commun.*, **11**, 651 (2010); https://doi.org/10.1016/j.catcom.2010.01.015
29. D. Chougule, K. Patil, P. Desai, A. Sawant and S. Sawant, *Int. J. Sci. Res. Eng. Manag.*, **7**, 1 (2023).
30. Y.R. Mejía and N.K. Reddy Bogireddy, *RSC Adv.*, **12**, 18661 (2022); https://doi.org/10.1039/D2RA02663E
31. R. Kore, A. Sawant and R. Rogers, *ACS Sustain. Chem.& Eng.*, **9**, 8797 (2021); https://doi.org/10.1021/acssuschemeng.1c01803
32. A. Sawant, D. Raut, N. Darvatkar, U. Desai and M. Salunkhe, *Catal. Commun.*, **12**, 273 (2010); https://doi.org/10.1016/j.catcom.2010.10.004
33. S. Jagadale, A. Teli, S. Kalake, A. Sawant, A. Yadav and P. Patil, *J. Electroanal. Chem.*, **816**, 99 (2018); https://doi.org/10.1016/j.jelechem.2018.01.059
34. S. Jagadale, A. Sawant, P. Patil, D. Patil, A. Mulik, D. Chandam, S. Sankpal and M. Deshmukh, *J. Heterocycl. Chem.*, **52**, 468 (2015); https://doi.org/10.1002/jhet.1958
35. S. Agnihotri, G. Bajaj, S. Mukherji and S. Mukherji, *Nanoscale*, **7**, 7415 (2015); https://doi.org/10.1039/C4NR06913G
36. O. Karvekar, P. Sarvalkar, A. Vadanagekar, R. Singhan, S. Jadhav, M. Nimbalkar and N. Prasad, *Appl. Nanosci.*, **12**, 2207 (2022); https://doi.org/10.1007/s13204-022-02470-1
37. P. Sarvalkar, A. Jamadar, S. Kakade, A. Magdum, P. Pawar, J. Yadav, M. Nimbalkar, N. Prasad, A. Ramteke and K. Sharma, *Results Eng.*, **22**, 102094 (2024); https://doi.org/10.1016/j.rineng.2024.102094
38. F. Lin and R. Doong, *J. Phys. Chem. C*, **115**, 6591 (2011); https://doi.org/10.1021/jp110956k